Wind project Ragnies

New Wind SPRL

Simple Engineering Assessment RADAR

Intersoft Electronics Services
services@intersoft-electronics.com
IES-22055

Version Control

Date	Status	Authority	Signature
19 Jun 22 v0.1	Draft	Reinhard Vermeulen Service Technician	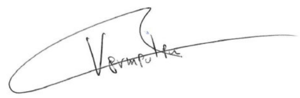
21 Jun 22 v1.0	Review and Approval	Robrecht Rosseel, ir. Technical lead	

Contents

1. List of Abbreviations

LoS .... Line of Sight

BAF .... Belgian Air Force

MoD .... Ministry of Defence

SEA .... Simple Engineering Assessment

SRTM .... Shuttle Radar Topography Mission

AGL .... Above Ground Level

AMSL .... Above Mean Sea level

RADAR ..... Radio Detection and Ranging

WT .... Wind Turbine

MTI .... Moving Target Indication

MTD .... Moving Target Detector

STC .... Sensitivity Time Control

CFAR .... Constant False Alarm Rate

ASR .... Airfield Surveillance Radar

PSR .... Primary Surveillance Radar

SSR .... Secondary Surveillance Radar

Pd .... Probability of Detection

RCS .... Radar Cross Section

dBsm .... Decibel Per Square Meter [$10 \log_{10} (\frac{RCS}{m^2})$]

VCC .... Vertical Clutter Canceller

RF .... Radio Frequency

RAG .... Range-Azimuth Gating

2. Introduction

Wind development located within line of sight of radar systems (LoS) can cause clutter and interference resulting in significant performance degradation. As wind turbines continue to be installed (more and bigger), and as advances in wind energy technology enable wind farms to be deployed in new regions of the country, the probability for wind development to present conflicts with radar missions related to air traffic control, weather forecasting, homeland security, and national defense is also likely to increase, as is the potential severity of those conflicts.

2.1 Wind turbine project

The project on behalf of **New Wind SPRL** concerns the following proposed wind turbines located near **Ragnies**, all coordinates are in Lambert72, the dimensions in this table are the maximum dimensions for this project (worst case scenario from radar point of view):

Turbine	X	Y	Height	Hub Height
WT01	145580	110094	180m	115m
WT02	145339	109608	180m	115m
WT03	145830	109562	180m	115m
WT04	145388	109110	180m	115m

Table 2.1: Turbines under test.

The turbines under test are visualised in the picture below.

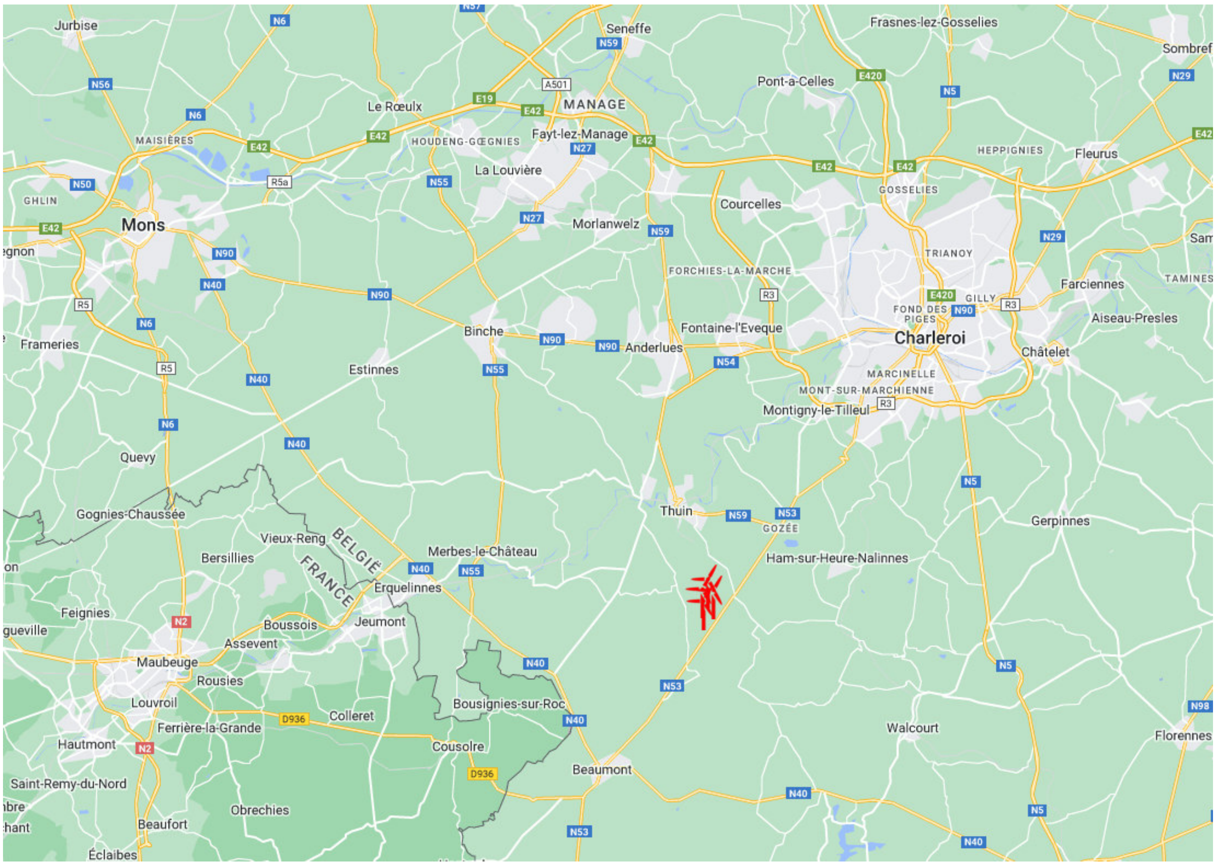

Figure 2.1: Geographic presentation of the turbines under test.

The turbines in table 2.1 will be studied taking into account a possible cumulative effect from wind turbines already installed or permitted near the turbines under test.

Taking into account the location and height of the turbines , a SEA for the Saint-Hubert and Florennes radars is required. An overview of the distances between these turbines and the Saint-Hubert and Florennes radars are given in tables 2.2 and 2.3.

Turbine	**Saint-Hubert [m]**
WT01	85456
WT02	85518
WT03	85040
WT04	85306

Table 2.2: Distance between the turbines under test and the Saint-Hubert radar.

Turbine	Florennes [m]
WT01	26233
WT02	26298
WT03	25819
WT04	26093

Table 2.3: Distance between the turbines under test and the Florennes radar.

2.2 Radar specifications

The radar specifications that are taken into account are listed below, table 2.4 and 2.5. The parameters have been provided or confirmed by the Belgian Ministry of Defence. The technical details have been omitted due to reasons of confidentiality.

ASR Saint-Hubert technical specifications
MTI
MTD
Median filter
Soft STC
VCC
CFAR
Range - Azimuth cell
Rotation speed
Instrumented range
Beam Width
Pulse compression
Wavelength

Table 2.4: ASR Saint-Hubert technical specifications.

ASR Florennes technical specifications
MTI
MTD
CFAR
Range - Azimuth cell
Rotation speed
Instrumented range
Beam Width
Pulse compression
Wavelength

Table 2.5: ASR Florennes technical specifications.

3. Scope

3.1 Eurocontrol requirements

Given that the project lies beyond 15km of the radar under assessment and in radar line of sight, MoD asks to perform a "Simple Assessment" (zone 3 in the figure below). This assessment, as detailed in section 4.3 of the EUROCONTROL [1] document, should be sufficient to enable the surveillance data provider to assess the situation.

Zone	**Zone 1**	**Zone 2**	**Zone 3**	**Zone 4**
Description	0 - 500 m	500 m - 15 km and in radar line of sight	Further than 15 km but within maximum instrumented range **and in** radar line of sight	Anywhere within maximum instrumented range but **not in** radar line of sight or outside the maximum instrumented range.
Assessment Requirements	**Safeguarding**	**Detailed assessment**	**Simple assessment**	**No assessment**

A Secondary Surveillance Radar (SSR) assessment is out of scope for this study.

The scope for this project **New Wind SPRL, Ragnies** is thus as follows:

Impact	Reference [1]	Radar	
		Saint-Hubert	Florennes
PSR probability of detection	4.3.1	✓	✓
PSR false target reports	4.3.2	✓	✓
PSR processing overload	4.3.3	✓	✓

Figure 3.1: Scope of the study.

The general way of executing the SEA has been confirmed by MoD without remarks [7].

3.2 Obstacles in the vicinity

In this assessment we take into account surrounding obstacles such as other wind turbines to evaluate the combined impact. For this we use an approximate 5-10 km radius. In this project, 13 other turbines have been identified, for more details see appendix A. These obstacles represent the worst case global effect with information coming from the IES database. These obstacles are a combination of existing turbines, permitted turbines and turbines in other permission processes.

The positioning of the turbines can be seen in the figure below. The black turbines represents the obstacles surrounding the turbines under test, which are symbolised by the red turbines .

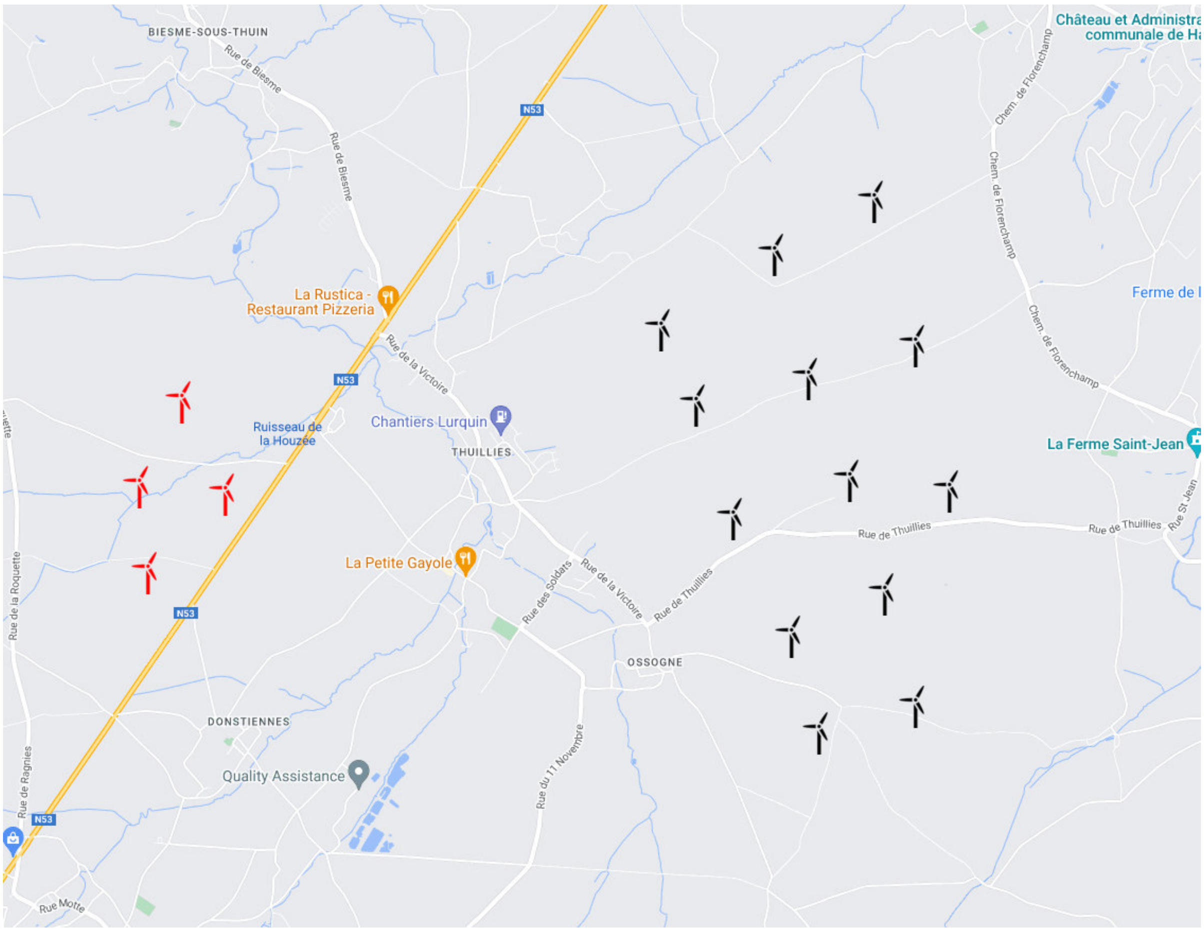

Figure 3.2: Obstacles around the turbines under test.

4. Simple Engineering Assessment SRE-M6 Saint-Hubert

A PSR simple engineering assessment is defined in the EUROCONTROL document to consist out of 3 parts, see also chapter 3 of this document:

- PSR probability of detection
- PSR false target reports
- PSR processing overload

Each of these items will be discussed in detail below. A geographic overview of the turbines under test and the defined obstacles is given below, figure 4.1. In red we see the new turbines and in black the defined obstacles. The black radar figure represents the Saint-Hubert SRE-M6 radar.

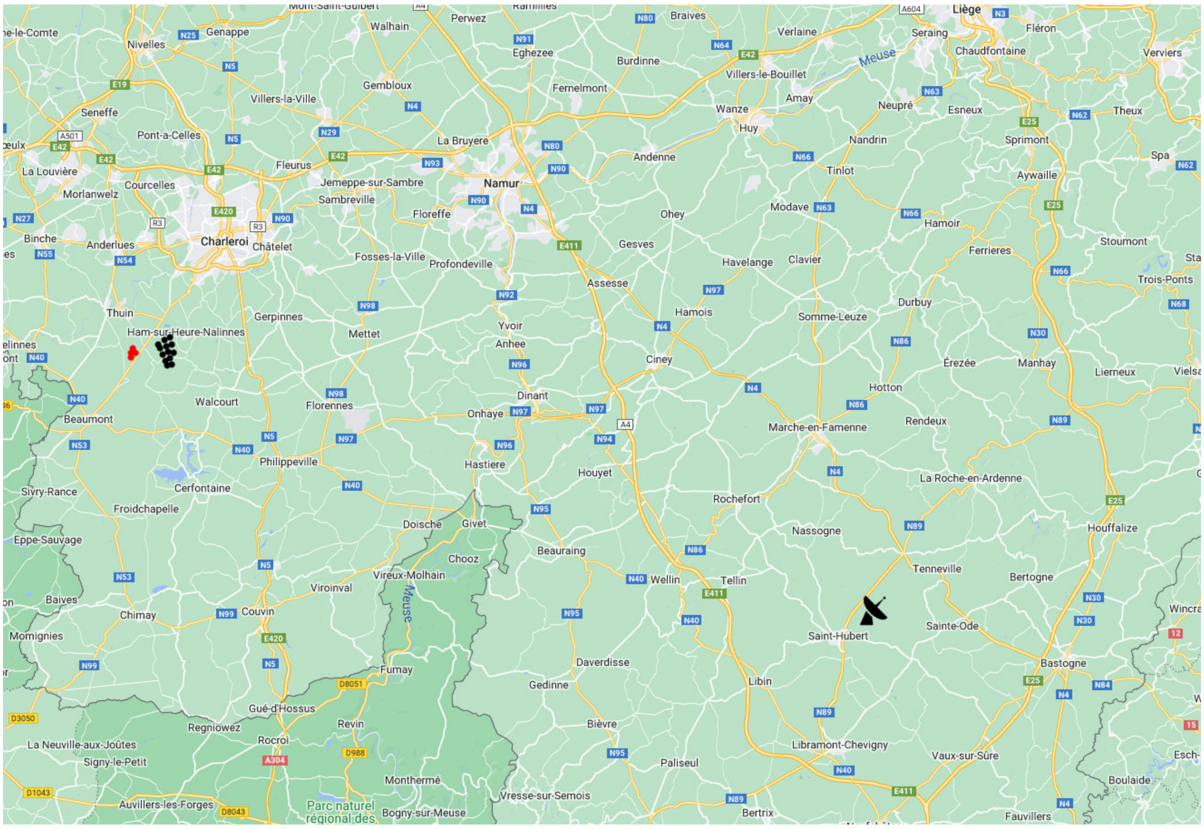

Figure 4.1: General overview relative to the Saint-Hubert radar.

4.1 PSR Probability of detection

Shadow regions behind the turbines

When a turbine lies directly between the transmitting and receiving antenna, the strength of the signal reaching the receiver is lower than it would otherwise be. For a radar system, this is the case for every obstacle that is within line of sight. The shadow region gives an indication of the severity of this effect. For the calculations we took into account the 4/3 earth model.

Shadow Height

First we look into the shadow height. We compare the shadow height of the turbines with the shadow generated by the terrain (SRTM [6]), a schematic representation is given in figure 4.2. These calculations are based on screening with an optical model for the propagation of the electromagnetic rays.

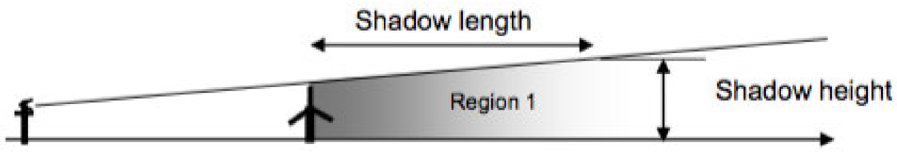

Figure 4.2: Schematic representation of the shadow height.

The closer the turbines to the radar system, the bigger the expected impact. For the turbines under test (table 2.1) we obtain the following results; figure 4.3.

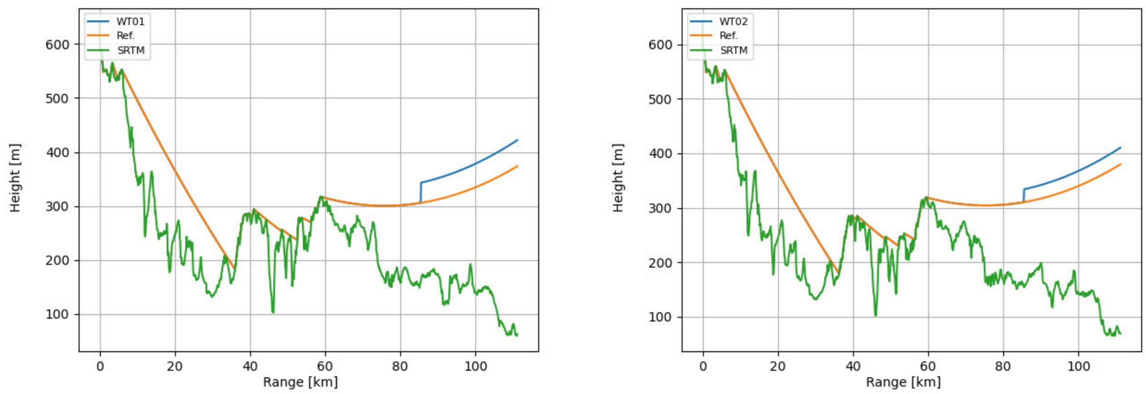

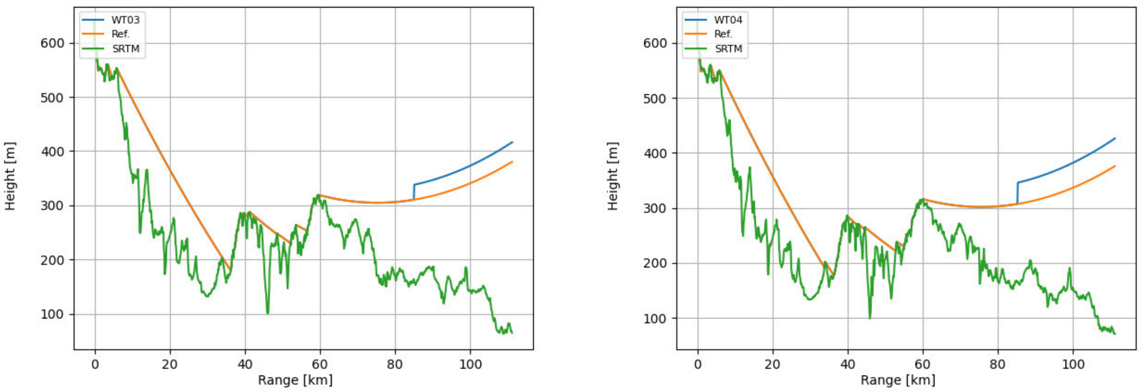

Figure 4.3: Shadow height Saint-Hubert radar, full instrumental range.

	Terrain shadow	**Turbine shadow**	**Difference**
WT01	337	372	35
WT02	341	367	25
WT03	341	375	34
WT04	337	380	42

Table 4.1: Shadow height comparison.

Partial conclusion: We notice that the wind turbines under test generate an additional shadow in the vertical dimension. At 100km this difference is about 34m or 10% compared to the current terrain shadow. This calculation gives us the worst case scenario, in reality this additional effect will be much smaller due to building obstructions and specific wave effects. The shadow zone is a region where the electromagnetic field is weaker when compared to a zone without obstructions (free space), so this zone is not completely dark. Due to the limited visibility of the turbines under test, the shadowing effects will be negligible.

Shadow Width

Similar to the shadow height we can calculate the shadow width which occurs due to the blocking of the radar signal in the azimuthal plane. The "signal blocking" is caused by destructive interference behind the turbines due to forward scattering effects.

A schematic overview is given in the figure below:

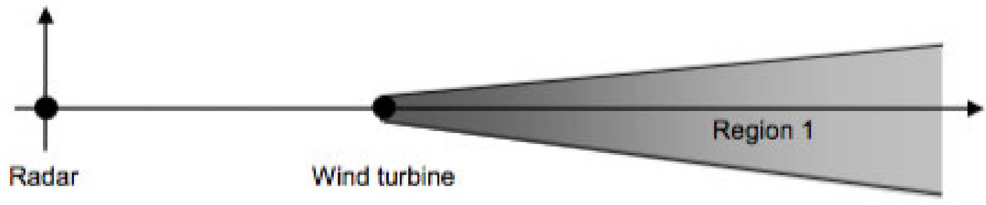

Figure 4.4: Schematic representation of the shadow width.

The shadow width depends on the addition of the signal in phase and anti-phase. If we calculate this for the three first *Fresnel zones* where destructive interference occurs (n = 1, 3 or 5) we obtain the results in figure 4.5. Since the relative difference in distance between the radar and all turbines is only small, all of the shadow width zones can be considered equal, thus only 1 is represented.

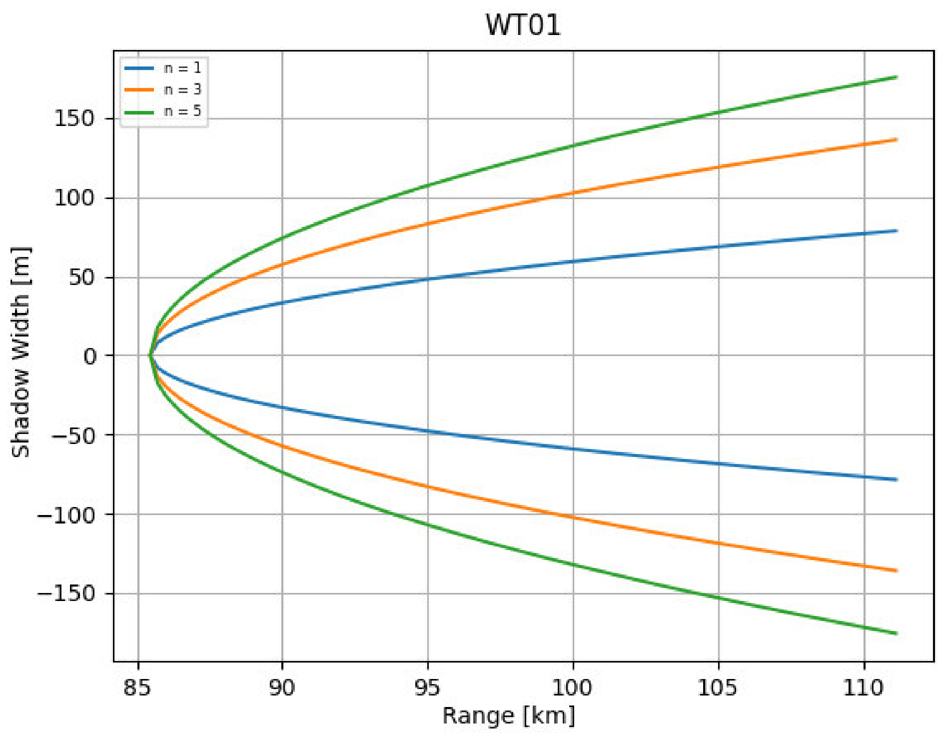

Figure 4.5: Actual representation of the shadow width for different Fresnel zones.

Partial conclusion: We notice that the wind turbines under test generate an additional shadow width zone. In reality, the shadow zone will not extend until the full instrumental range but will only occur the first kilometers behind the turbines. The additional shadow width zone will merge with the shadow zones of the existing/permitted turbines.
In the shadow width region, the effects are caused by destructive interference between the radar signal and the forward scattered signal coming from the wind turbines. Due to the weaker signal coming from forward scattering of the turbines only a reduction in

power will be measured in these zones, not a complete loss of signal. This effect will be the strongest in the first Fresnel zone (n = 1) and will be almost undetectable in the 3rd relevant Fresnel zone (n = 5). Due to the large difference in intensity between the forward scatter and the direct waves, the effect will only be noticeable close to the turbines.

Raised threshold above and around the turbines

The possible large reflections of wind turbines raise the detector threshold of the radar, which lowers the probability of detection of a target. The size of the region depends on the CFAR algorithm installed, as specified in section 2.2.

Given the size of a range cell, we calculate that a wind turbine can potentially influence the radar threshold ±810 meters from its position. Combined with the beam width and distance to the turbines under test we obtain the following impacted zones, see figure 4.6.

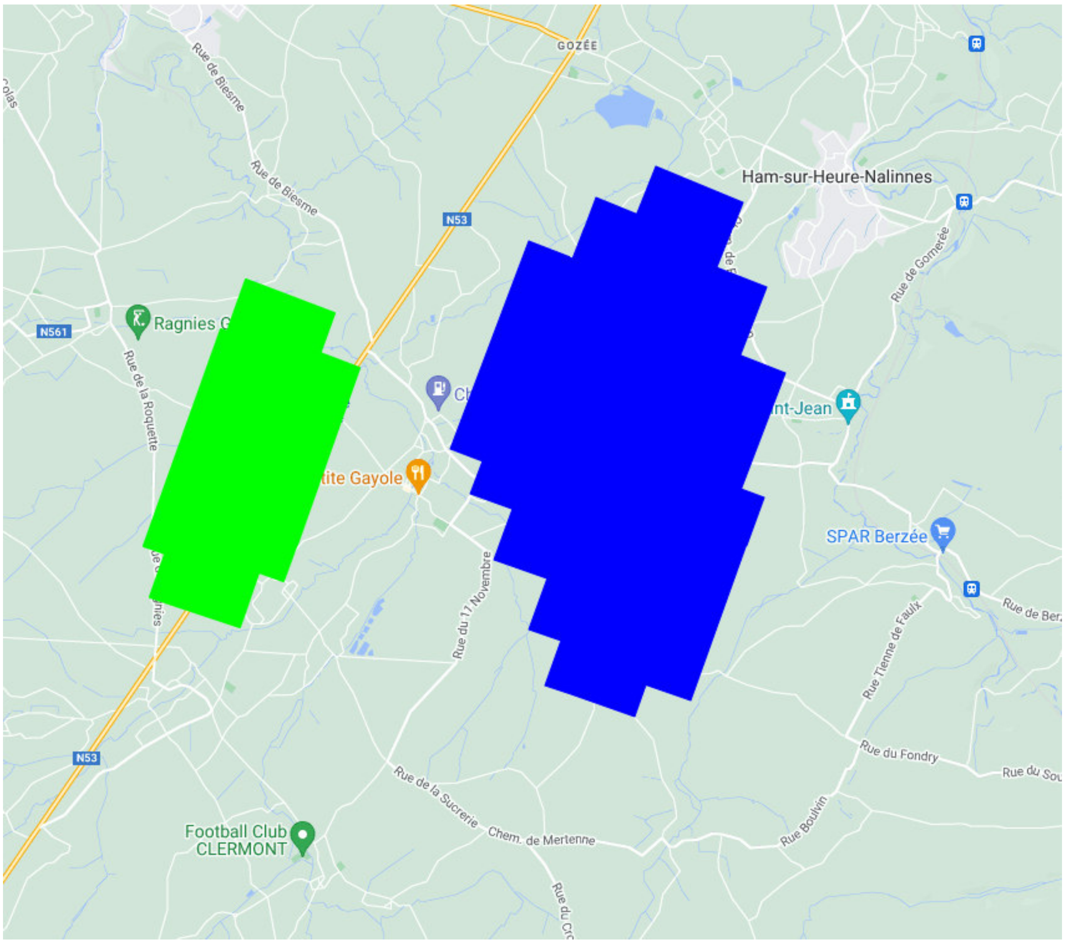

Figure 4.6: Schematic representation of the Saint-Hubert radar CFAR zones.

If we compare the blue area (existing obstacles) with the green area (new CFAR impacted area), we can see a netto increase of the CFAR impacted region, the numbers are given in table 4.2. There is no overlap between the raised threshold zone of the turbines under test and the raised threshold zones of existing/permitted turbine. A cumulative effect of about 3dB will be present between the raised threshold zones of the turbines under test.

CFAR Area calculation	
Area before	11.1 km^2
Area after	15.2 km^2
Difference	4.1 km^2
Difference	37%

Table 4.2: CFAR area increase.

For the RCS of the turbines under test different values have been used. In real life this will also be the case, depending on the wind direction and blade speed of the turbines. Even within one complete blade revolution this RCS value can vary by a factor of 10,000. A simplified statistical overview is given in the table below, 4.3 [4].

Monostatic RCS L-band			
Maximum	Mean	Median	Minimum
37 dBsm	27 dBsm	27 dBsm	0 dBsm

Table 4.3: Stochastic representation of monostatic RCS turbines, L-band.

For this study we analysed the impact on the raised threshold above and around the turbines for RCS values of 10, 15, 20, 25, 30 and 35 dBsm to simulate all possible scenarios. Next we calculated the impact on a target right above the turbines (worst case) at different altitudes. The target size is simulated as 0 dBsm ($1m^2$).

If the reflected power of the target remains above the detection threshold, it can still be seen by the radar system. In these calculations we processed the impact of MTI/MTD and the beam pattern. A schematic overview of our test set-up can be seen below:

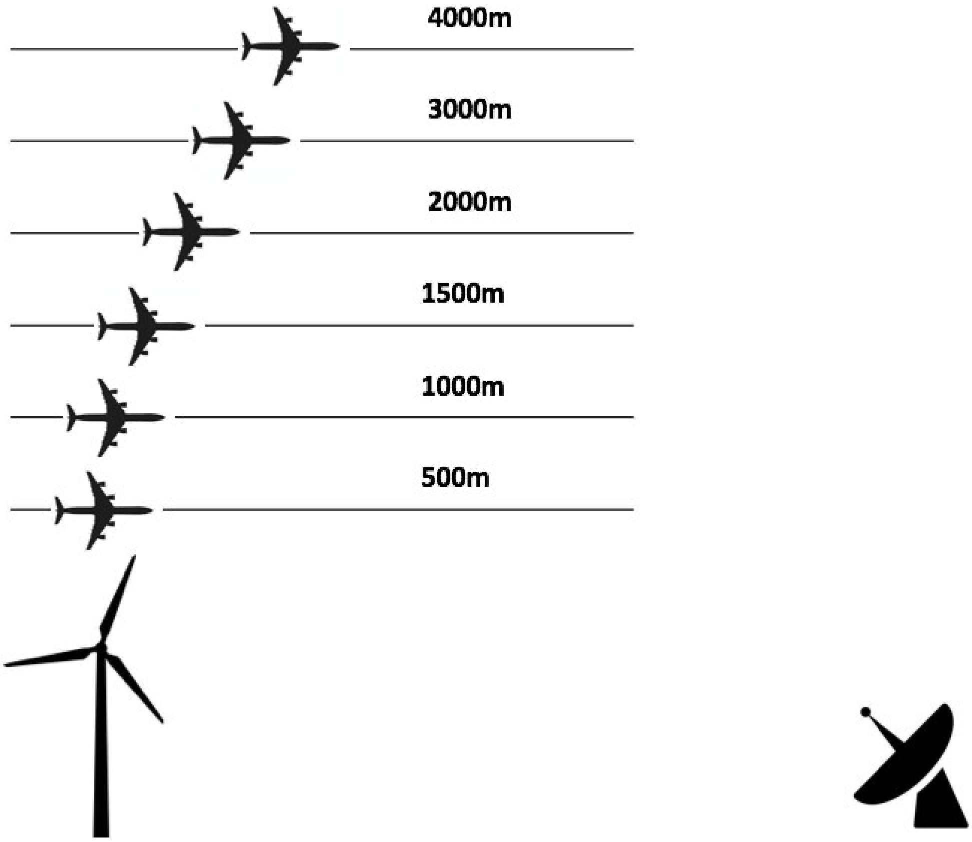

Figure 4.7: Schematic representation of the CFAR test set-up.

To give an idea about the expected RCS of the turbines under test we perform a simplified RCS calculation. In this calculation we only take into account the part of the turbines that is visible for the radar system. As detailed simulations have shown, the turbine masts are the dominant contributors to the monostatic RCS, regardless of the orientation of the rotor [8].

We notice that due to the terrain screening (Fig. 4.3), the mast of the turbines will not be visible for the Saint-Hubert radar. Only a part of the contribution of the rotor will be present. The effective RCS of the wind turbines under test will be below 15dBsm.

Taking into account the cumulative effect, the total impact on the CFAR algorithm is about 18dBsm.
To present the case for the Saint-Hubert radar we display the results for a WT RCS of 20, 25, 30 and 35dBsm. For the complete results, see annex B.

WT	Beam	Reference	500m	1000m	1500m	2000m	3000m	4000m
WT01	1.0	-128.0[dBw]	-130.1	-125.3	-120.5	-117.0	-114.5	-118.6
WT01	2.0	-136.0[dBw]	-137.4	-132.2	-126.9	-122.8	-116.5	-115.1
WT02	1.0	-128.0[dBw]	-130.2	-125.3	-120.5	-117.0	-114.5	-118.6
WT02	2.0	-136.0[dBw]	-137.4	-132.2	-126.9	-122.9	-116.5	-115.1
WT03	1.0	-128.0[dBw]	-130.1	-125.2	-120.4	-116.9	-114.4	-118.5
WT03	2.0	-136.0[dBw]	-137.3	-132.1	-126.8	-122.8	-116.4	-115.0
WT04	1.0	-128.0[dBw]	-130.1	-125.3	-120.4	-117.0	-114.4	-118.5
WT04	2.0	-136.0[dBw]	-137.4	-132.2	-126.9	-122.8	-116.5	-115.0

Table 4.4: Detection of a 0 dBsm target at different altitudes (RCS$_{WT}$= 20dBsm).

WT	Beam	Reference	500m	1000m	1500m	2000m	3000m	4000m
WT01	1.0	-123.0[dBw]	-130.1	-125.3	-120.5	-117.0	-114.5	-118.6
WT01	2.0	-131.0[dBw]	-137.4	-132.2	-126.9	-122.8	-116.5	-115.1
WT02	1.0	-123.0[dBw]	-130.2	-125.3	-120.5	-117.0	-114.5	-118.6
WT02	2.0	-131.0[dBw]	-137.4	-132.2	-126.9	-122.9	-116.5	-115.1
WT03	1.0	-123.0[dBw]	-130.1	-125.2	-120.4	-116.9	-114.4	-118.5
WT03	2.0	-131.0[dBw]	-137.3	-132.1	-126.8	-122.8	-116.4	-115.0
WT04	1.0	-123.0[dBw]	-130.1	-125.3	-120.4	-117.0	-114.4	-118.5
WT04	2.0	-131.0[dBw]	-137.4	-132.2	-126.9	-122.8	-116.5	-115.0

Table 4.5: Detection of a 0 dBsm target at different altitudes (RCS$_{WT}$= 25dBsm).

WT	Beam	Reference	500m	1000m	1500m	2000m	3000m	4000m
WT01	1.0	-118.0[dBw]	-130.1	-125.3	-120.5	-117.0	-114.5	-118.6
WT01	2.0	-126.0[dBw]	-137.4	-132.2	-126.9	-122.8	-116.5	-115.1
WT02	1.0	-118.0[dBw]	-130.2	-125.3	-120.5	-117.0	-114.5	-118.6
WT02	2.0	-126.0[dBw]	-137.4	-132.2	-126.9	-122.9	-116.5	-115.1
WT03	1.0	-118.0[dBw]	-130.1	-125.2	-120.4	-116.9	-114.4	-118.5
WT03	2.0	-126.0[dBw]	-137.3	-132.1	-126.8	-122.8	-116.4	-115.0
WT04	1.0	-118.0[dBw]	-130.1	-125.3	-120.4	-117.0	-114.4	-118.5
WT04	2.0	-126.0[dBw]	-137.4	-132.2	-126.9	-122.8	-116.5	-115.0

Table 4.6: Detection of a 0 dBsm target at different altitudes (RCS$_{WT}$= 30dBsm).

WT	Beam	Reference	500m	1000m	1500m	2000m	3000m	4000m
WT01	1.0	-113.0[dBw]	-130.1	-125.3	-120.5	-117.0	-114.5	-118.6
WT01	2.0	-121.0[dBw]	-137.4	-132.2	-126.9	-122.8	-116.5	-115.1
WT02	1.0	-113.0[dBw]	-130.2	-125.3	-120.5	-117.0	-114.5	-118.6
WT02	2.0	-121.0[dBw]	-137.4	-132.2	-126.9	-122.9	-116.5	-115.1
WT03	1.0	-113.0[dBw]	-130.1	-125.2	-120.4	-116.9	-114.4	-118.5
WT03	2.0	-121.0[dBw]	-137.3	-132.1	-126.8	-122.8	-116.4	-115.0
WT04	1.0	-113.0[dBw]	-130.1	-125.3	-120.4	-117.0	-114.4	-118.5
WT04	2.0	-121.0[dBw]	-137.4	-132.2	-126.9	-122.8	-116.5	-115.0

Table 4.7: Detection of a 0 dBsm target at different altitudes (RCS_{WT}= 35dBsm).

The 'Reference' column in the tables above state the value of the reflected power coming from the turbines after applying all mitigations (and CFAR) present in the radar. The overflying targets can only be detected if the returned power is larger than this reference value.

We notice for a turbine with a RCS of 20-25dBsm (tables 4.4 and 4.5) that overflying targets with a RCS of 0dBsm will be seen up from an altitude of 1000-1500m AMSL when flying above or near the wind turbines. When the wind turbine has a reflection of 30dBsm or 35dBsm (tables 4.6 and 4.7) the small airplane will only be visible above 2000-3000m AMSL.

Partial conclusion: As the radar of Saint-Hubert has no automatic mitigations installed, the impact on the CFAR could be considerable. For a turbine reflectivity of 20dBsm the small objects flying above will be visible above 1000m AMSL. A RCS of 25dBsm, 30dBsm and 35dBsm will reduce the visibility for the smallest targets in the lower altitude ranges. This is not the case in this project. The expected RCS impact on the CFAR algorithm is about 18dBsm. As only the top (rotor) part of the turbine under test will be visible, small aircrafts will remain visible.

Impact on signal processing

The impact on the signal processing will be a general rise of data to be processed, with the current technology used in radar systems this impact will be negligible, the only real impact will be the CFAR processing.

4.2 PSR false target reports

Modern surveillance radars are equipped with multiple mechanisms to obtain detections of flying targets only. To suppress reflections at non-moving objects (stator), adaptive cluttermaps are maintained within each doppler bin.

A flying target will be detected if its reflection exceeds the risen CFAR threshold in its range-azimuth cell. This has been discussed in section 4.1. Since the turbines under test are only partially visible, no false targets will be present.

4.3 PSR processing overload

The extra video processing as a result of the wind turbines under test is negligible in comparison with the radar technology used. The impact on the signal processing will be a general rise of data to be processed, with the current technology used in radar systems this impact will be negligible.

4.4 Practical analysis

The technology of the Saint-Hubert radar makes it possible to export the clutter maps of the system. In the region of the wind project, one turbine is already present (as described in section 3.2). The turbines under test are located at 46NM from the radar at an azimuth of 290.6°.

The Saint-Hubert system uses frequency interleaving, only one clutter combination is presented below due to the similarities between both. The clutter maps for the low beam are visualised in figures 4.8 and 4.9, the clutter maps for the high beam are visualised in figures 4.10 and 4.11.

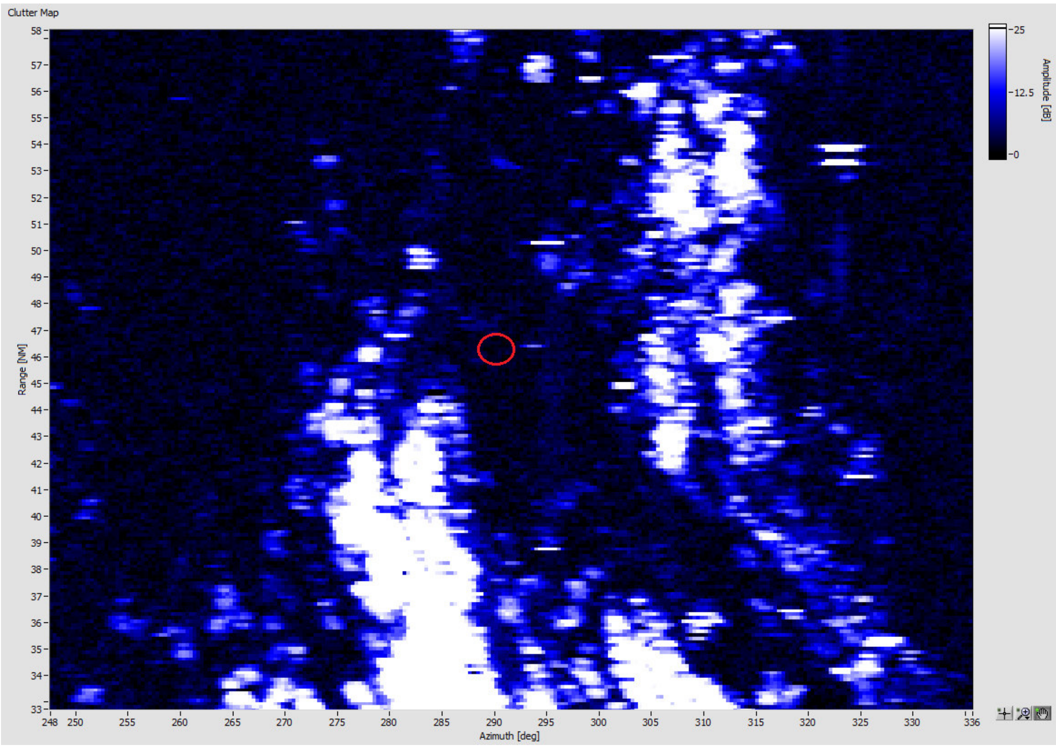

Figure 4.8: Clutter map of the Saint-Hubert radar (low beam - Doppler bin 0).

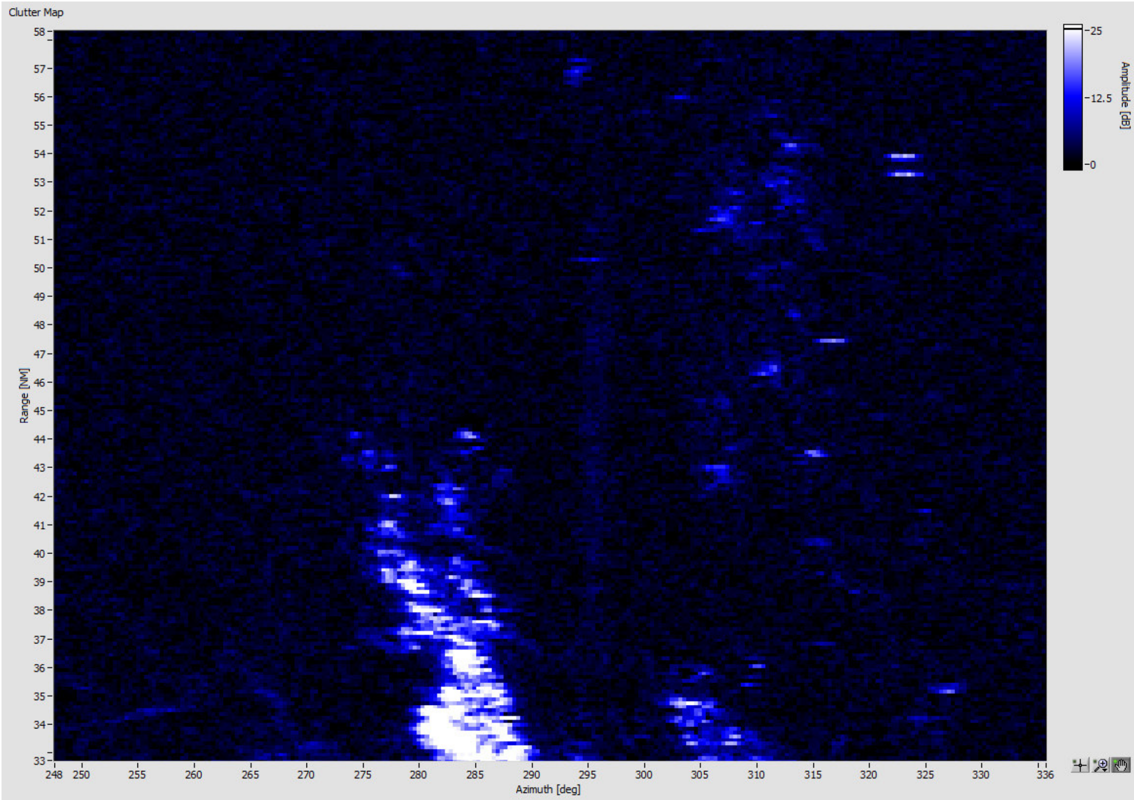

Figure 4.9: Clutter map of the Saint-Hubert radar (low beam - Doppler bin 4).

In the low beam - bin 0 we notice a lot of clutter zones at different ranges and azimuth positions, this indicates the good positioning of the radar - at the highest point in the region, able to see very low altitudes.

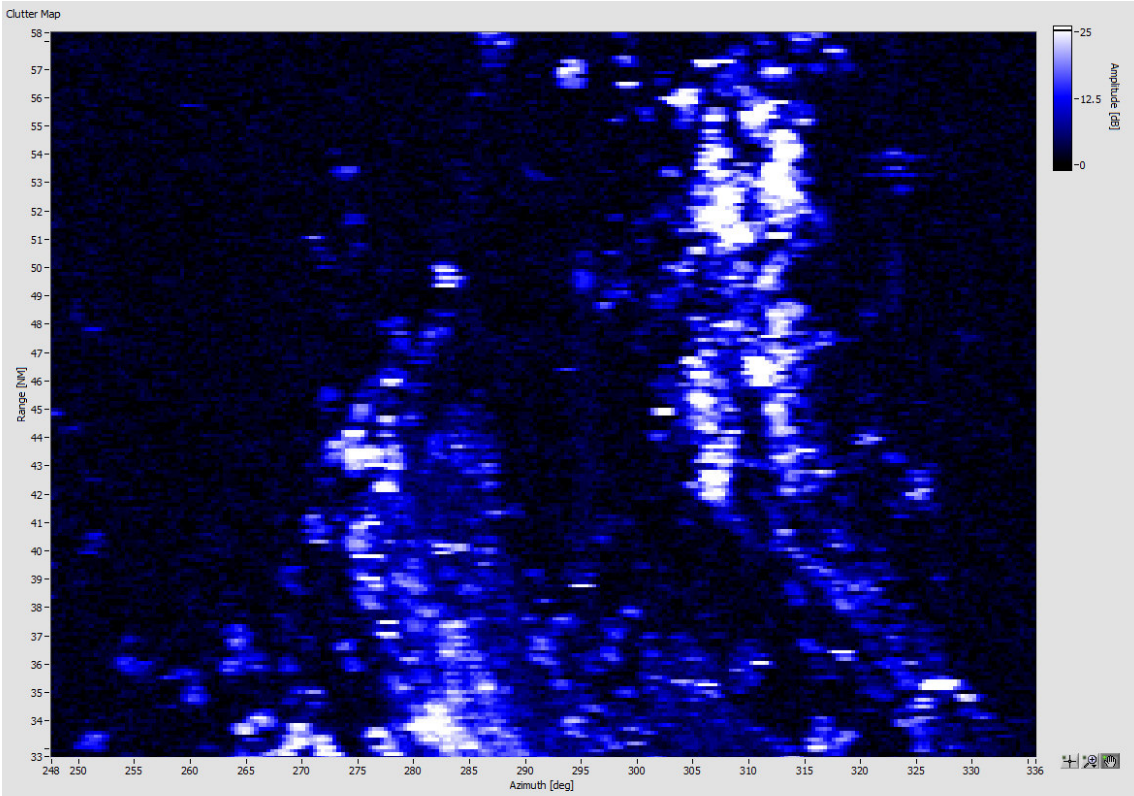

Figure 4.10: Clutter map of the Saint-Hubert radar (high beam - Doppler bin 0).

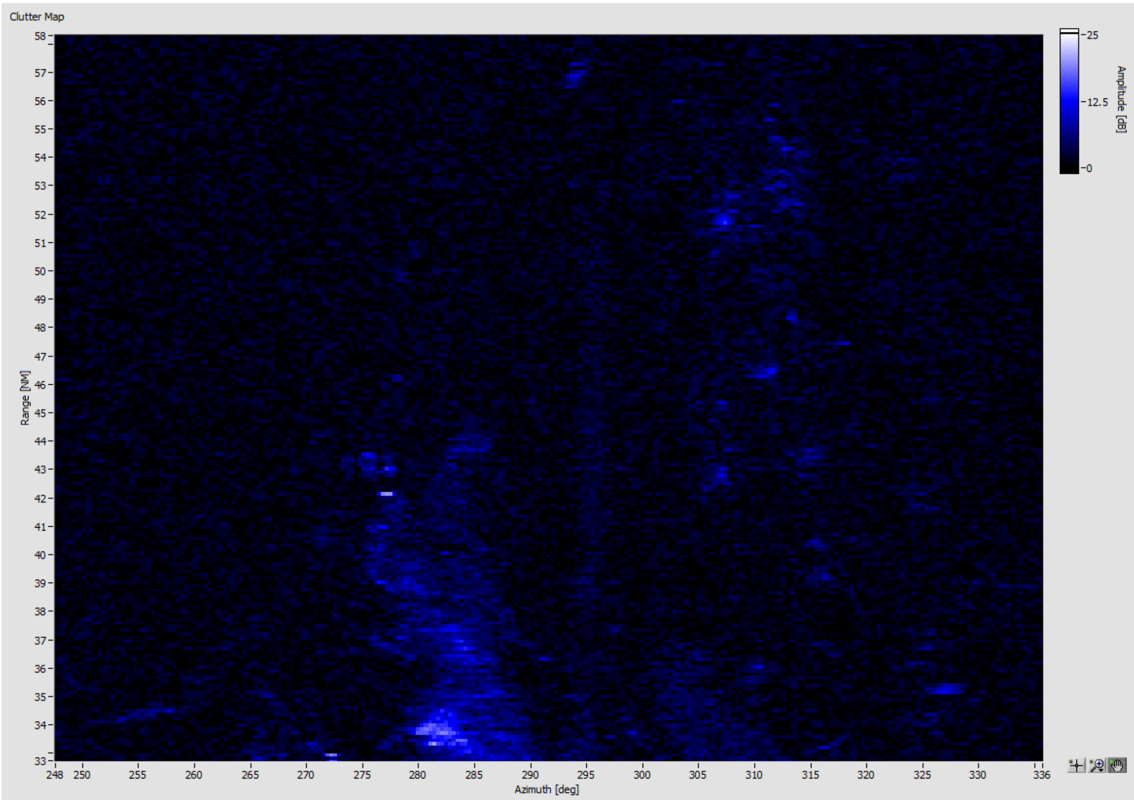

Figure 4.11: Clutter map of the Saint-Hubert radar (high beam - Doppler bin 4).

Clutter is present in Doppler bin 0 of the low beam of the Saint-Hubert radar near the location of the turbines under test. The impact of these zones on the system is important for the generation of false plots and the detection performance. In higher doppler bins (Fig. 4.9), the high peaks are no longer present. In the extended region of the turbines under test, RAG and VCC have been applied to some cells (not visible). RAG (Range Azimuth Gating), together with VCC, are the main mitigation options available. The existing turbines show a small signature in the cluttermap. Due to the relative large distance and large portion off terrain screening, the impact on the radar will remain limited to none. A similar effect is to be expected from the turbines under test.

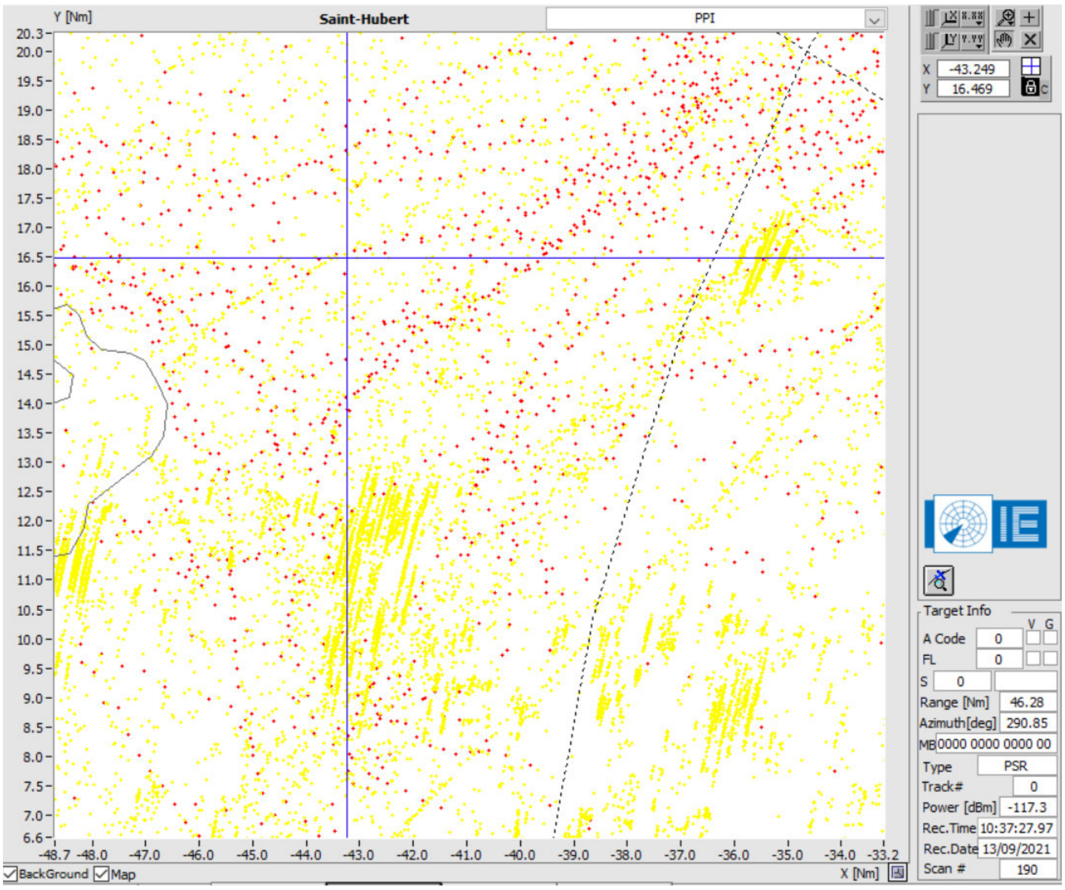

Figure 4.12: False plots in the vicinity of the Turbines under test.

The false plots in the region are shown in figure 4.12, the blue marker is placed on the location of the turbines under test. The yellow dots represent the false primitive reports that are filtered out by the signal processing, the pink dots represent the PSR "true" plots. Currently, no false plots cluster are generated in the region of the turbines under test. They are not to be expected after the construction of this project.

In Figure 4.13 the marker is placed in the vicinity of the turbines under test, current Pd in the region is 90%. The parameters of the RCM can be found in annex C.1.

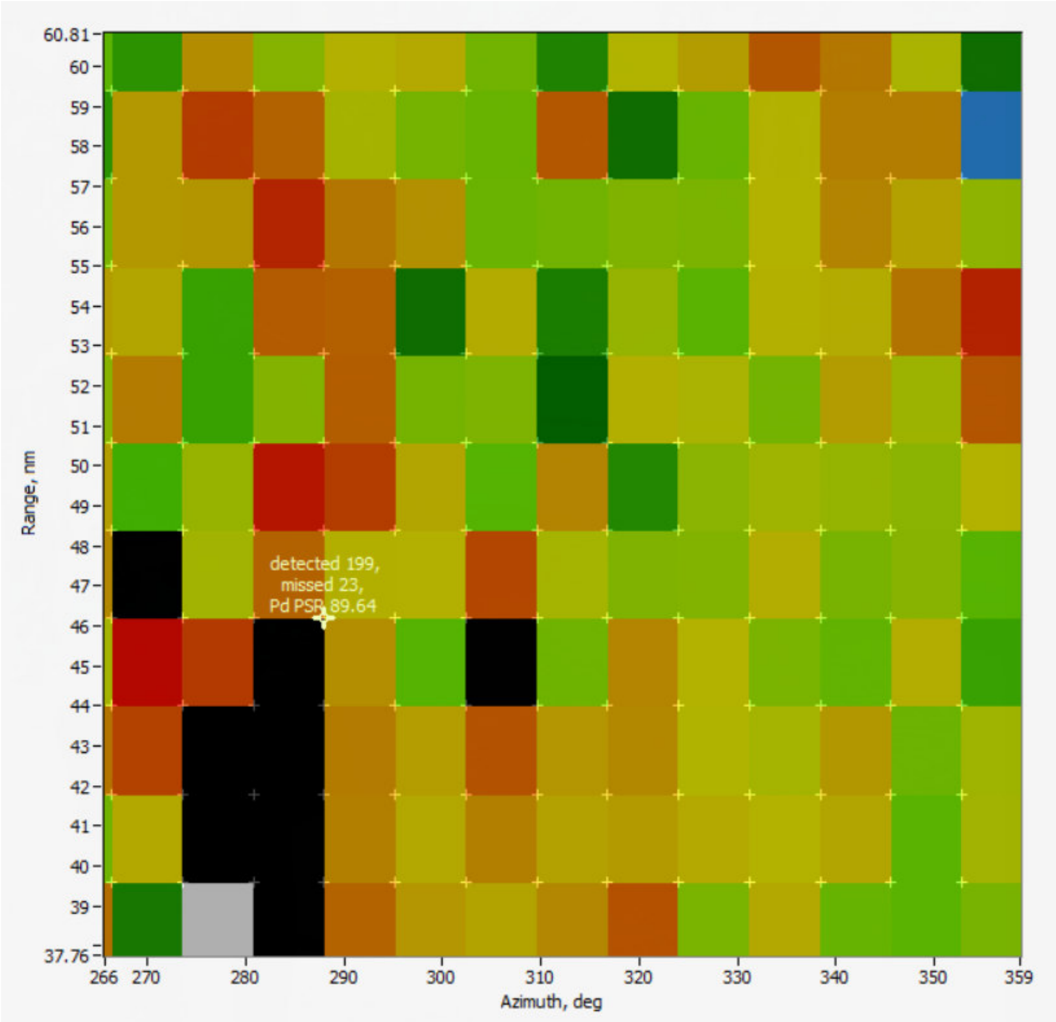

Figure 4.13: visualisation of the Pd in the Vicinity of the turbines under test.

4.5 Mitigations

Section 4.1 and 4.4 show that there will be almost no impact on the detection near and above the turbines under test. Next to this, false plots (Section 4.2) will not be present.

5. Simple Engineering Assessment STAR 2000 Florennes

A PSR simple engineering assessment is defined in the EUROCONTROL document to consist out of 3 parts, see also chapter 3 of this document:

- PSR probability of detection
- PSR false target reports
- PSR processing overload

Each of these items will be discussed in detail below. A geographic overview of the turbines under test and the defined obstacles are given below, figure 5.1. In red we see the turbines under test, in black the defined obstacles. The black radar figure represents the Florennes Airport Surveillance radar.

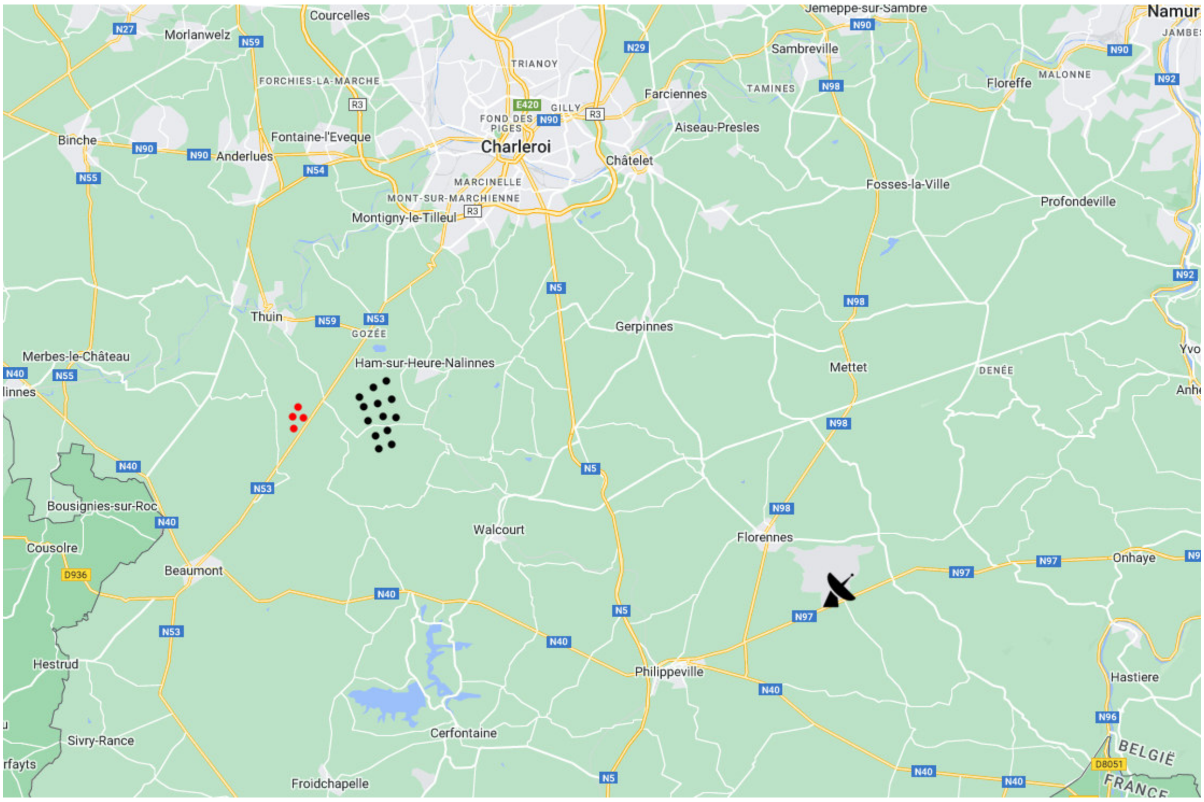

Figure 5.1: General overview relative to the Florennes radar.

5.1 PSR Probability of detection

Shadow regions behind the turbines

When a turbine lies directly between the transmitting and receiving antenna, the strength of the signal reaching the receiver is lower than it would otherwise be. For a radar system, this is the case for every obstacle that is within line of sight. The shadow region gives an indication of the severity of this effect. For the calculations we took into account the 4/3 earth model.

Shadow Height

First we look into the shadow height. We compare the shadow height of the turbines with the shadow generated by the terrain (SRTM [6]), a schematic representation is given in figure 5.2. These calculations are based on screening with an optical model for the propagation of the electromagnetic rays.

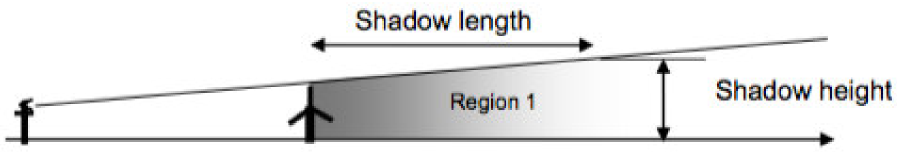

Figure 5.2: Schematic representation of the shadow height

The closer the turbine to the radar system, the bigger the expected impact. For the turbines under test (table 2.1) we obtain the following results; figure 5.3.

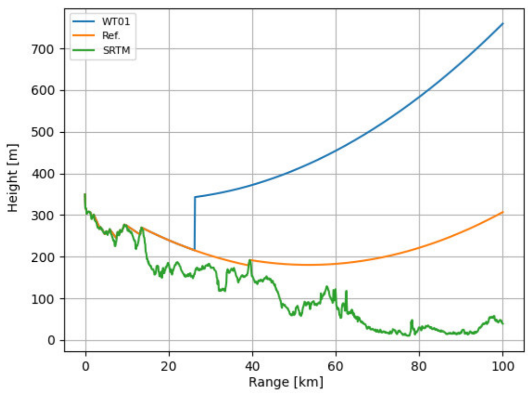

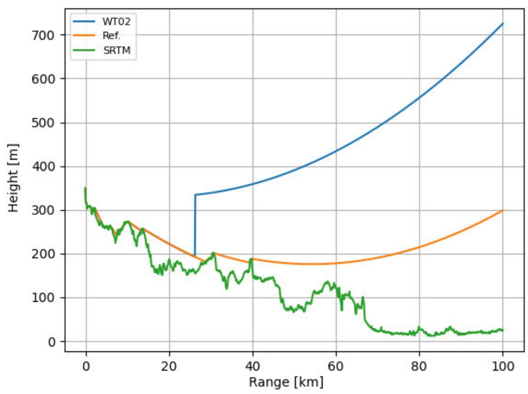

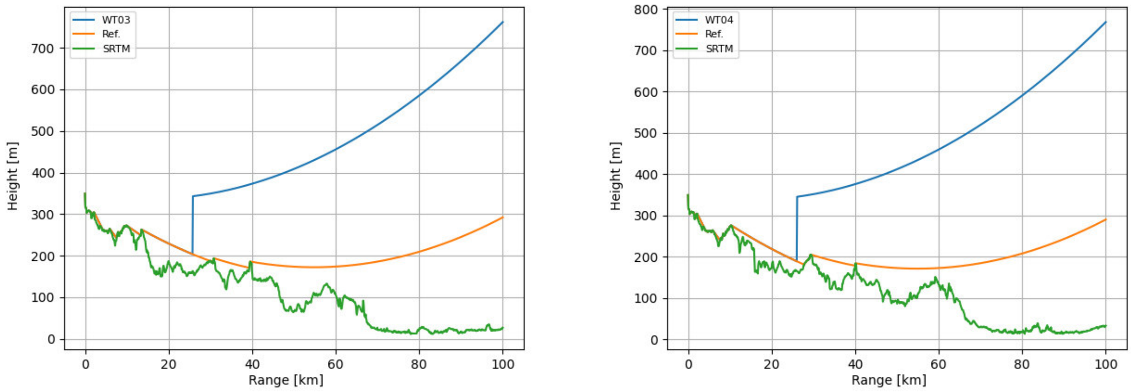

Figure 5.3: Shadow height Florennes radar, full instrumental range.

	Terrain shadow	**Turbine shadow**	**Difference**
WT01	307	759	452
WT02	298	725	426
WT03	292	761	469
WT04	289	768	478

Table 5.1: Shadow height comparison.

Partial conclusion: We notice that the wind turbines under test generate an additional shadow in the vertical dimension. At 100km this difference is 456m (153%) compared to the current terrain shadow. This calculation gives us the worst case scenario, in reality this additional effect will be much smaller due to building obstructions and specific wave effects. The shadow zone is a region where the electromagnetic field is weaker when compared to a zone without obstructions (free space), so this zone is not completely dark. Due to the small fraction of the terrain screening, the shadowing effect will be considerable the first kilometers behind the turbines.

Shadow Width

Similar as the shadow height we can calculate the shadow width which occurs due to the blocking of the radar signal in the azimuthal plane. The "signal blocking" is caused by destructive interference behind the turbine due to forward scattering effects.

A schematic overview is given in the figure below:

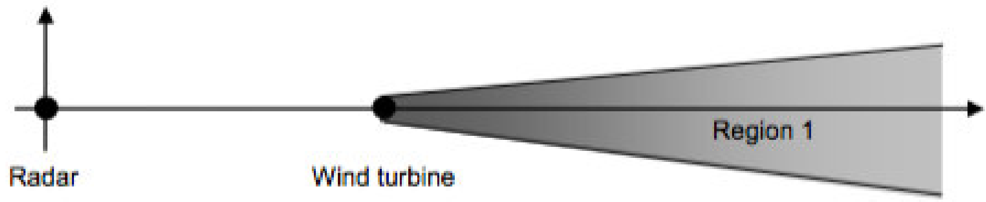

Figure 5.4: Schematic representation of the shadow width.

The shadow width depends from the addition of the signal in phase and anti-phase. If we calculate this for the three first *Fresnel zones* where destructive interference occurs (n = 1, 3 or 5) we obtain the results in figure 5.5. Since the relative difference in distance between the radar and all turbines is only small, all of the shadow width zones can be considered equal, thus only 1 is represented.

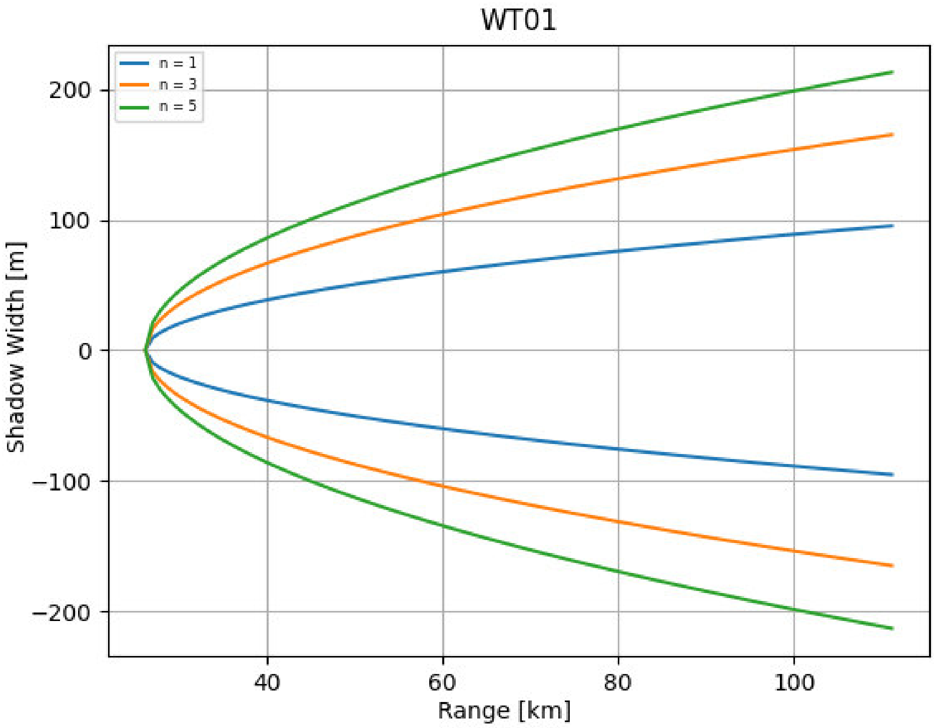

Figure 5.5: Actual representation of the shadow width for different Fresnel zones.

Partial conclusion: We notice that the wind turbines under test generate an additional shadow width zone. In reality, the shadow zone will not extend until the full instrumental range but will only occur the first kilometers behind each turbine. The additional shadow width zone will combine with the shadow zones of the existing/permitted turbines.

In the shadow width region, the effects are caused by destructive interference between the radar signal and the forward scattered signal coming from the wind turbine. Due to the weaker signal coming from forward scattering of the turbines only a reduction in power will be measured in these zones, not a complete loss of signal. This effect will be the strongest in the first Fresnel zone (n = 1) and will be almost undetectable in the 3rd relevant Fresnel zone (n=5). Due to the large difference in intensity between the forward scatter and the direct waves, the effect will only be noticeable close to the turbines under test.

Raised threshold above and around the turbines

The possible large reflections of wind turbines raise the detector threshold of the radar, which lowers the probability of detection of a target. The size of the region depends on the CFAR algorithm installed, as specified in section 2.2.

Given the size of a range cell, we calculate that a wind turbine can potentially influence the radar threshold ±1080 meters from its position. Combined with the beam width and distance to the turbines under test we obtain the following impacted zones, see figure 5.6.

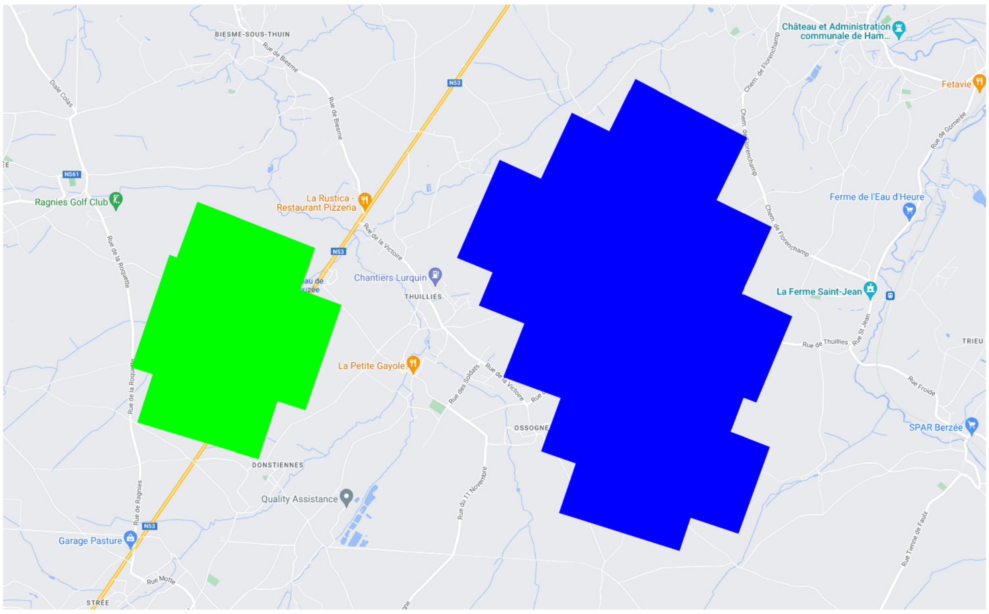

Figure 5.6: Schematic representation of the Florennes radar CFAR zones.

If we compare the blue area (existing obstacles only) with the green area (new CFAR impacted area), we can see a netto increase of the CFAR impacted region, the numbers are given in table 5.2. There is a no overlap between the CFAR zones of turbine under test with the permitted/existing turbines. A cumulative effect of about 3dB will be present in the zone with the overlap between the turbines under test.

CFAR Area calculation	
Area before	8.2 km^2
Area after	11.1 km^2
Difference	2.9 km^2
Difference	35%

Table 5.2: CFAR area increase.

For the RCS of the turbines under test different values have been used. In real life this will also be the case, depending on the wind direction and blade speed of the turbines. Even within one complete blade revolution this RCS value can vary by a factor of 10,000. A simplified statistic overview is given in the table below, 5.3 [4].

Monostatic RCS S-band			
Maximum	Mean	Median	Minimum
37 dBsm	27 dBsm	27 dBsm	0 dBsm

Table 5.3: Stochastic representation of monostatic RCS turbines, S-band.

For this study we analysed the impact on the raised threshold above and around the turbines for RCS values of 10, 15, 20, 25, 30 and 35 dBsm to simulate all possible scenarios. Next we calculated the impact on a target right above the turbines (worst case) at different altitudes. The target size is simulated as 0 dBsm ($1m^2$).

If the reflected power of the target remains above the detection threshold, it can still be seen by the radar system. In these calculations we processed the impact of MTI/MTD and the beam pattern. A schematic overview of our test set-up can be seen below:

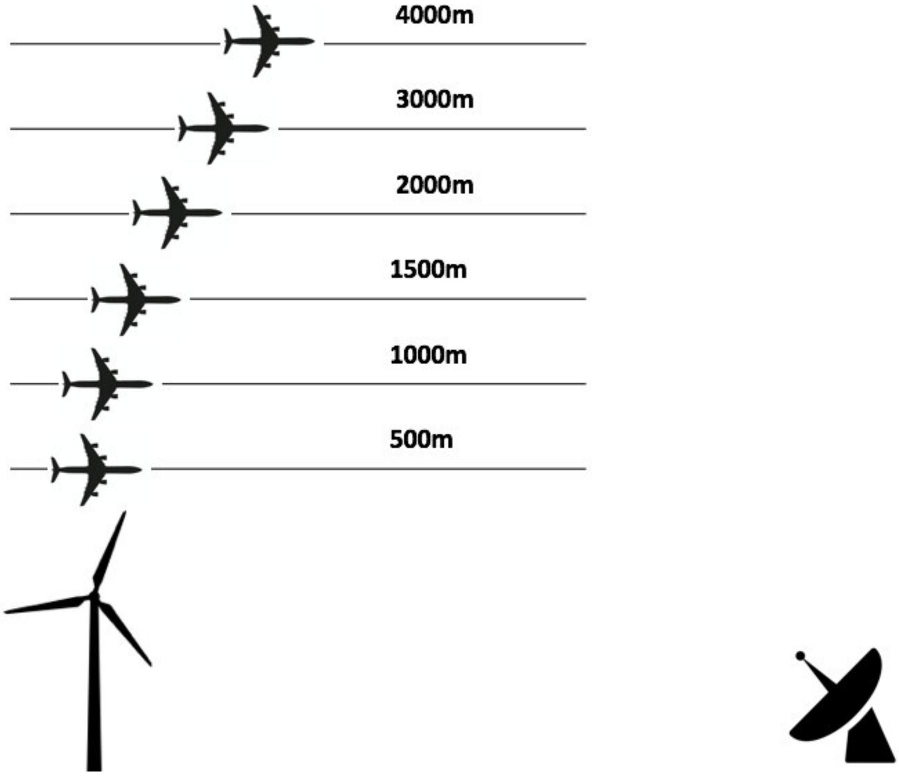

Figure 5.7: Schematic representation of the CFAR test set-up.

To give an idea about the expected RCS of the turbines under test we usually perform a simplified RCS calculation. In this calculation we only take into account the part of the turbines that is visible for the radar system. As detailed simulations have shown, the turbine masts are the dominant contributors to the monostatic RCS, regardless of the orientation of the rotor [8].

The mast has been simulated as a frustum and we calculated its monostatic RCS in relation to the different relevant EM incident angles. The results are displayed below, figure 5.8. Because of the similarity between the turbines under test only the graph of the first turbine has been displayed.

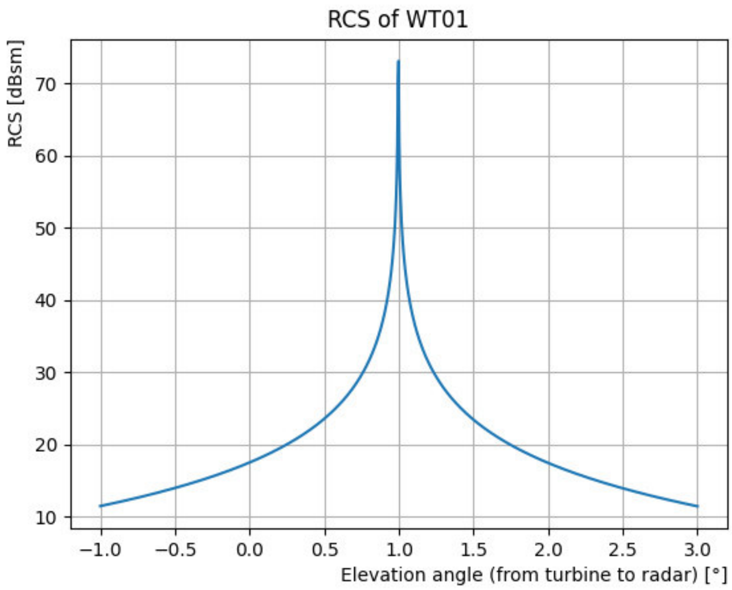

Figure 5.8: Monostatic RCS of the turbine under test at different elevation angles.

	Elevation Angle [°]	**RCS S-band [dBsm]**
E1	0.3798	21.7
E2	0.4229	22.3
E3	0.4041	22.0
E4	0.4387	22.5

Table 5.4: Overview monostatic RCS simulation of the turbines under test.

A worst case average value of 22.5dBsm for the mast can be taken into account. This RCS value represents the ideal scenario in which no fluctuation losses occur (also known as Swerling). In reality the RCS will vary in strength. When adding the RCS of the rotor (15dBsm), the complete turbine monostatic RCS is about 23.2dBsm.

Taking into account the cumulative effect, the total impact on the CFAR algorithm is about 26.2dBsm.

To present the case for the Florennes radar we display the results for a WT RCS of 15 and 20 dBsm. For the complete results, see annex B.

WT	**Beam**	**Reference**	**500m**	**1000m**	**1500m**	**2000m**	**3000m**	**4000m**
WT01	1.0	-94.0[dBw]	-96.7	-97.4	-99.2	-100.1	-101.9	-103.2
WT01	2.0	-103.0[dBw]	-104.2	-102.0	-100.2	-99.5	-99.6	-101.1
WT02	1.0	-94.0[dBw]	-96.8	-97.4	-99.2	-100.1	-101.8	-103.2
WT02	2.0	-103.0[dBw]	-104.3	-102.1	-100.2	-99.6	-99.6	-101.1
WT03	1.0	-93.0[dBw]	-96.5	-97.2	-98.9	-99.9	-101.7	-102.9
WT03	2.0	-103.0[dBw]	-103.9	-101.7	-99.9	-99.3	-99.4	-100.9
WT04	1.0	-93.0[dBw]	-96.6	-97.3	-99.1	-100.1	-101.8	-103.1
WT04	2.0	-103.0[dBw]	-104.1	-101.9	-100.1	-99.4	-99.5	-101.1

Table 5.5: Detection of a 0 dBsm target at different altitudes (RCS_{WT}= 15dBsm).

WT	**Beam**	**Reference**	**500m**	**1000m**	**1500m**	**2000m**	**3000m**	**4000m**
WT01	1.0	-89.0[dBw]	-96.7	-97.4	-99.2	-100.1	-101.9	-103.2
WT01	2.0	-98.0[dBw]	-104.2	-102.0	-100.2	-99.5	-99.6	-101.1
WT02	1.0	-89.0[dBw]	-96.8	-97.4	-99.2	-100.1	-101.8	-103.2
WT02	2.0	-98.0[dBw]	-104.3	-102.1	-100.2	-99.6	-99.6	-101.1
WT03	1.0	-88.0[dBw]	-96.5	-97.2	-98.9	-99.9	-101.7	-102.9
WT03	2.0	-98.0[dBw]	-103.9	-101.7	-99.9	-99.3	-99.4	-100.9
WT04	1.0	-88.0[dBw]	-96.6	-97.3	-99.1	-100.1	-101.8	-103.1
WT04	2.0	-98.0[dBw]	-104.1	-101.9	-100.1	-99.4	-99.5	-101.1

Table 5.6: Detection of a 0 dBsm target at different altitudes (RCS_{WT}= 20dBsm).

The 'Reference' column in the tables above state the value of the reflected power coming from the turbine after applying all mitigations (and CFAR) present in the radar. The overflying targets can only be detected if the returned power is larger than this reference value.

We notice for a turbine with a RCS of 15dBsm (table 5.5) that overflying targets with a RCS of 0dBsm will be seen from an approximate altitude of 1000m AMSL when flying above or near the wind turbine. When the wind turbine has a reflection of 20dBsm (table 5.6) the small airplane will be invisible for the radar.

Partial conclusion: As the radar of Florennes has no automatic mitigations installed, the impact on the CFAR will be considerable. For a turbine reflectivity of 15dBsm the small objects flying above will be visible above 1000m AMSL. For a turbine reflectivity of 20dBsm the smallest targets are no longer visible. The expected RCS impact on the CFAR algorithm is about 26.2dBsm. This is the worst case scenario with the cumulative effect taken into account. The smallest targets will be hard to detect, regular aircraft will have a larger RCS and will be easier to detect, but not during all scans.

Impact on signal processing

The impact on the signal processing will be a general rise of data to be processed, with the current technology used in radar systems this impact will be negligible, the only real impact will be the CFAR processing.

5.2 PSR false target reports

Modern surveillance radars are equipped with multiple mechanisms to obtain detections of flying targets only. To suppress reflections at non-moving objects (stator), adaptive cluttermaps are maintained within each doppler bin.

A flying target will be detected if its reflection exceeds the risen CFAR threshold in its range-azimuth cell. This has been discussed in section 5.1. Since the RCS of the turbine under test will vary over time, even within a single rotation, false targets can be present if no mitigations are applied.

5.3 PSR processing overload

The extra video processing as a result of the wind turbines under test is negligible in comparison with the radar technology used, see also section 5.1, impact on the signal processing.

5.4 Practical analysis

The technology of the Florennes STAR 2000 radar makes it not possible to export the clutter maps of the system. In the region of the wind project, several turbines are already present (as described in section 3.2). The turbine is located at 14-15NM from the radar at an azimuth of 288-290°.

5.5 Mitigations

Section 5.1 shows that there will be an impact on the detection near and above the turbine under test. Next to this, false plots (Section 5.2) could be present during some scans.

To reduce or eliminate the possible negative effects of the turbines under test, zone blanking needs to be investigated in the region of the turbines once the installation is completed. This is however a very severe mitigation technique as all information in these cells is lost. This method should only be used as a last resort.

The STAR 2000 at Florennes has the WFF (Wind Farm Filter) installed which will help to rebuild the tracks faster after a loss of detection near wind turbines or prevent new tracks building up due to the effects of wind turbines. This is also called "Non-Auto Initiation Areas/Zones (NAIAs/NAIZs)". This analysis (at tracker level) is however out of scope for this study.

More effective mitigation solutions at RF level include RAG (for each beam separately) and VCC for the higher beam(s). This will however only be available after **an upgrade of the current radar system with the NGSP® solution** [5] which includes wind farm mitigation processing soft-and hardware. With VCC the impact of the turbine under test can be diminished with at least 20dB . After VCC, no significant operational impact should remain.

6. Conclusion

Saint-Hubert

Limited Shadow width and height effects will be present for the Saint-Hubert radar, these can impact the PSR probability of detection. However, due to the large portion of terrain screening, these effects are negligible.

An impact will occur on the CFAR processing due to the fact that no automatic windmill mitigation is installed. The limited visibility of the turbines under test from the Saint-Hubert radar will reduce this effect. Small targets will be easily detected for RCS values of the wind turbines up to 30dBsm, from 35dBsm and higher, the smallest targets will be harder to detect (above 2000m AMSL). More details can be found in the study and Annex B. The expected cumulative RCS of the turbines under test will be around 18dBsm.

No PSR processing overload or PSR false target reports are to be expected.

From both the theoretical and practical analysis, very limited impact is expected in the region of the turbines under test, no after installation assessment is required.

Florennes

Shadow width and height effects are present for the Florennes radar, these can impact the PSR probability of detection. However, due to the existing turbines at similar distances, these effects are already present without consequences on the operationality of the radar.

The shadow height will limit itself to the part of the turbines under test which is higher than the surrounding obstacles. The relative raise of the shadow height (153%) will be limited due to wave effects. The shadow width zone is limited in width and only a reduction in intensity will be noticeable, this zone is not completely dark.

An impact will occur on the CFAR processing due to the fact that no automatic windmill mitigation is installed. Small targets will be easily detected for RCS values of the wind turbine up to 15dBsm, from 20dBsm and higher, the smallest targets will be harder or impossible to detect. Small targets close to the turbines under test will be invisible during most scans, depending on the RCS value of the target. The expected cumulative RCS of the turbines under test will be around 26.2dBsm.

PSR false target reports are to be expected depending on the orientation of the turbine rotor.

No PSR processing overload is to be expected.

From the theoretical analysis, a considerable impact is expected in the region of the turbines under test. In order to reduce or eliminate the negative effects, an upgrade of the system may need to be envisaged with the NGSP® solution. The NGSP hardware contains the RAG and VCC mitigation solutions.

Bibliography

[1] Frank BRENNER, *EUROCONTROL Guidelines for Assessing the Potential Impact on Wind turbine on Surveillance Sensors*, GUID-130, Edition 1.2, Sept 2014.

[2] Merrill Skolnik, *RADAR handbook*, Third edition

[3] Marcel Vanuytven, *Octrooi WO 2010/037770*, 08/04/2010

[4] Gavin J Poupart, *Wind farms impact on radar aviation - Final report*, DTI PUB URN 03/1294, September 2003

[5] Intersoft Electronics, Next Generation Signal Processor (NGSP), `https://intersoft-electronics.com/technology_components_ngsp.html`, 2021

[6] U.S. Geological Survey, `https://dds.cr.usgs.gov`, August 2020

[7] Vincent De Smet *RE: Engineering studie BAF* 13/03/2018

[8] ScientificWorldJournal, *Simplified Formulae for the Estimation of Offshore Wind Turbines Clutter on Marine Radars.*, March 2017

Appendices

A. Turbines in the vicinity

Turbine	Lambert X	Lambert Y	Height
Z1	148348	110506	150m
Z2	149001	110938	150m
Z3	149575	111247	150m
Z4	148545	110073	150m
Z5	149198	110227	150m
Z6	149812	110413	150m
Z7	148763	109424	150m
Z8	149436	109640	150m
Z9	150010	109578	150m
Z10	149099	108744	150m
Z11	149634	108991	150m
Z12	149258	108188	150m
Z13	149812	108343	150m

B. Impact on the CFAR

This chapter gives the estimated returned power of a reference target of 0dBsm and compares this to the incident power coming from the wind turbine after all of the data processing (CFAR, VCC, MTD, ...) This makes it possible to check from which altitudes a small aircraft can be detected.

B.1 Saint-Hubert

B.1.1 WT RCS 10 dBsm

WT	Beam	Threshold	500m	1000m	1500m	2000m	3000m	4000m
WT01	1.0	-138.0[dBw]	-130.1	-125.3	-120.5	-117.0	-114.5	-118.6
WT01	2.0	-146.0[dBw]	-137.4	-132.2	-126.9	-122.8	-116.5	-115.1
WT02	1.0	-138.0[dBw]	-130.2	-125.3	-120.5	-117.0	-114.5	-118.6
WT02	2.0	-146.0[dBw]	-137.4	-132.2	-126.9	-122.9	-116.5	-115.1
WT03	1.0	-138.0[dBw]	-130.1	-125.2	-120.4	-116.9	-114.4	-118.5
WT03	2.0	-146.0[dBw]	-137.3	-132.1	-126.8	-122.8	-116.4	-115.0
WT04	1.0	-138.0[dBw]	-130.1	-125.3	-120.4	-117.0	-114.4	-118.5
WT04	2.0	-146.0[dBw]	-137.4	-132.2	-126.9	-122.8	-116.5	-115.0

B.1.2 WT RCS 15 dBsm

WT	Beam	Threshold	500m	1000m	1500m	2000m	3000m	4000m
WT01	1.0	-133.0[dBw]	-130.1	-125.3	-120.5	-117.0	-114.5	-118.6
WT01	2.0	-141.0[dBw]	-137.4	-132.2	-126.9	-122.8	-116.5	-115.1
WT02	1.0	-133.0[dBw]	-130.2	-125.3	-120.5	-117.0	-114.5	-118.6
WT02	2.0	-141.0[dBw]	-137.4	-132.2	-126.9	-122.9	-116.5	-115.1
WT03	1.0	-133.0[dBw]	-130.1	-125.2	-120.4	-116.9	-114.4	-118.5
WT03	2.0	-141.0[dBw]	-137.3	-132.1	-126.8	-122.8	-116.4	-115.0
WT04	1.0	-133.0[dBw]	-130.1	-125.3	-120.4	-117.0	-114.4	-118.5
WT04	2.0	-141.0[dBw]	-137.4	-132.2	-126.9	-122.8	-116.5	-115.0

B.1.3 WT RCS 20 dBsm

WT	Beam	Threshold	500m	1000m	1500m	2000m	3000m	4000m
WT01	1.0	-128.0[dBw]	-130.1	-125.3	-120.5	-117.0	-114.5	-118.6
WT01	2.0	-136.0[dBw]	-137.4	-132.2	-126.9	-122.8	-116.5	-115.1
WT02	1.0	-128.0[dBw]	-130.2	-125.3	-120.5	-117.0	-114.5	-118.6
WT02	2.0	-136.0[dBw]	-137.4	-132.2	-126.9	-122.9	-116.5	-115.1
WT03	1.0	-128.0[dBw]	-130.1	-125.2	-120.4	-116.9	-114.4	-118.5
WT03	2.0	-136.0[dBw]	-137.3	-132.1	-126.8	-122.8	-116.4	-115.0
WT04	1.0	-128.0[dBw]	-130.1	-125.3	-120.4	-117.0	-114.4	-118.5
WT04	2.0	-136.0[dBw]	-137.4	-132.2	-126.9	-122.8	-116.5	-115.0

B.1.4 WT RCS 25 dBsm

WT	Beam	Threshold	500m	1000m	1500m	2000m	3000m	4000m
WT01	1.0	-123.0[dBw]	-130.1	-125.3	-120.5	-117.0	-114.5	-118.6
WT01	2.0	-131.0[dBw]	-137.4	-132.2	-126.9	-122.8	-116.5	-115.1
WT02	1.0	-123.0[dBw]	-130.2	-125.3	-120.5	-117.0	-114.5	-118.6
WT02	2.0	-131.0[dBw]	-137.4	-132.2	-126.9	-122.9	-116.5	-115.1
WT03	1.0	-123.0[dBw]	-130.1	-125.2	-120.4	-116.9	-114.4	-118.5
WT03	2.0	-131.0[dBw]	-137.3	-132.1	-126.8	-122.8	-116.4	-115.0
WT04	1.0	-123.0[dBw]	-130.1	-125.3	-120.4	-117.0	-114.4	-118.5
WT04	2.0	-131.0[dBw]	-137.4	-132.2	-126.9	-122.8	-116.5	-115.0

B.1.5 WT RCS 30 dBsm

WT	Beam	Threshold	500m	1000m	1500m	2000m	3000m	4000m
WT01	1.0	-118.0[dBw]	-130.1	-125.3	-120.5	-117.0	-114.5	-118.6
WT01	2.0	-126.0[dBw]	-137.4	-132.2	-126.9	-122.8	-116.5	-115.1
WT02	1.0	-118.0[dBw]	-130.2	-125.3	-120.5	-117.0	-114.5	-118.6
WT02	2.0	-126.0[dBw]	-137.4	-132.2	-126.9	-122.9	-116.5	-115.1
WT03	1.0	-118.0[dBw]	-130.1	-125.2	-120.4	-116.9	-114.4	-118.5
WT03	2.0	-126.0[dBw]	-137.3	-132.1	-126.8	-122.8	-116.4	-115.0
WT04	1.0	-118.0[dBw]	-130.1	-125.3	-120.4	-117.0	-114.4	-118.5
WT04	2.0	-126.0[dBw]	-137.4	-132.2	-126.9	-122.8	-116.5	-115.0

B.1.6 WT RCS 35 dBsm

WT	Beam	Reference	500m	1000m	1500m	2000m	3000m	4000m
WT01	1.0	-113.0[dBw]	-130.1	-125.3	-120.5	-117.0	-114.5	-118.6
WT01	2.0	-121.0[dBw]	-137.4	-132.2	-126.9	-122.8	-116.5	-115.1
WT02	1.0	-113.0[dBw]	-130.2	-125.3	-120.5	-117.0	-114.5	-118.6
WT02	2.0	-121.0[dBw]	-137.4	-132.2	-126.9	-122.9	-116.5	-115.1
WT03	1.0	-113.0[dBw]	-130.1	-125.2	-120.4	-116.9	-114.4	-118.5
WT03	2.0	-121.0[dBw]	-137.3	-132.1	-126.8	-122.8	-116.4	-115.0
WT04	1.0	-113.0[dBw]	-130.1	-125.3	-120.4	-117.0	-114.4	-118.5
WT04	2.0	-121.0[dBw]	-137.4	-132.2	-126.9	-122.8	-116.5	-115.0

B.2 Florennes

B.2.1 WT RCS 10 dBsm

WT	Beam	Reference	500m	1000m	1500m	2000m	3000m	4000m
WT01	1.0	-99.0[dBw]	-96.7	-97.4	-99.2	-100.1	-101.9	-103.2
WT01	2.0	-108.0[dBw]	-104.2	-102.0	-100.2	-99.5	-99.6	-101.1
WT02	1.0	-99.0[dBw]	-96.8	-97.4	-99.2	-100.1	-101.8	-103.2
WT02	2.0	-108.0[dBw]	-104.3	-102.1	-100.2	-99.6	-99.6	-101.1
WT03	1.0	-98.0[dBw]	-96.5	-97.2	-98.9	-99.9	-101.7	-102.9
WT03	2.0	-108.0[dBw]	-103.9	-101.7	-99.9	-99.3	-99.4	-100.9
WT04	1.0	-98.0[dBw]	-96.6	-97.3	-99.1	-100.1	-101.8	-103.1
WT04	2.0	-108.0[dBw]	-104.1	-101.9	-100.1	-99.4	-99.5	-101.1

B.2.2 WT RCS 15 dBsm

WT	Beam	Reference	500m	1000m	1500m	2000m	3000m	4000m
WT01	1.0	-94.0[dBw]	-96.7	-97.4	-99.2	-100.1	-101.9	-103.2
WT01	2.0	-103.0[dBw]	-104.2	-102.0	-100.2	-99.5	-99.6	-101.1
WT02	1.0	-94.0[dBw]	-96.8	-97.4	-99.2	-100.1	-101.8	-103.2
WT02	2.0	-103.0[dBw]	-104.3	-102.1	-100.2	-99.6	-99.6	-101.1
WT03	1.0	-93.0[dBw]	-96.5	-97.2	-98.9	-99.9	-101.7	-102.9
WT03	2.0	-103.0[dBw]	-103.9	-101.7	-99.9	-99.3	-99.4	-100.9
WT04	1.0	-93.0[dBw]	-96.6	-97.3	-99.1	-100.1	-101.8	-103.1
WT04	2.0	-103.0[dBw]	-104.1	-101.9	-100.1	-99.4	-99.5	-101.1

B.2.3 WT RCS 20 dBsm

WT	Beam	Reference	500m	1000m	1500m	2000m	3000m	4000m
WT01	1.0	-89.0[dBw]	-96.7	-97.4	-99.2	-100.1	-101.9	-103.2
WT01	2.0	-98.0[dBw]	-104.2	-102.0	-100.2	-99.5	-99.6	-101.1
WT02	1.0	-89.0[dBw]	-96.8	-97.4	-99.2	-100.1	-101.8	-103.2
WT02	2.0	-98.0[dBw]	-104.3	-102.1	-100.2	-99.6	-99.6	-101.1
WT03	1.0	-88.0[dBw]	-96.5	-97.2	-98.9	-99.9	-101.7	-102.9
WT03	2.0	-98.0[dBw]	-103.9	-101.7	-99.9	-99.3	-99.4	-100.9
WT04	1.0	-88.0[dBw]	-96.6	-97.3	-99.1	-100.1	-101.8	-103.1
WT04	2.0	-98.0[dBw]	-104.1	-101.9	-100.1	-99.4	-99.5	-101.1

B.2.4 WT RCS 25 dBsm

WT	Beam	Reference	500m	1000m	1500m	2000m	3000m	4000m
WT01	1.0	-84.0[dBw]	-96.7	-97.4	-99.2	-100.1	-101.9	-103.2
WT01	2.0	-93.0[dBw]	-104.2	-102.0	-100.2	-99.5	-99.6	-101.1
WT02	1.0	-84.0[dBw]	-96.8	-97.4	-99.2	-100.1	-101.8	-103.2
WT02	2.0	-93.0[dBw]	-104.3	-102.1	-100.2	-99.6	-99.6	-101.1
WT03	1.0	-83.0[dBw]	-96.5	-97.2	-98.9	-99.9	-101.7	-102.9
WT03	2.0	-93.0[dBw]	-103.9	-101.7	-99.9	-99.3	-99.4	-100.9
WT04	1.0	-83.0[dBw]	-96.6	-97.3	-99.1	-100.1	-101.8	-103.1
WT04	2.0	-93.0[dBw]	-104.1	-101.9	-100.1	-99.4	-99.5	-101.1

B.2.5 WT RCS 30 dBsm

WT	Beam	Reference	500m	1000m	1500m	2000m	3000m	4000m
WT01	1.0	-79.0[dBw]	-96.7	-97.4	-99.2	-100.1	-101.9	-103.2
WT01	2.0	-88.0[dBw]	-104.2	-102.0	-100.2	-99.5	-99.6	-101.1
WT02	1.0	-79.0[dBw]	-96.8	-97.4	-99.2	-100.1	-101.8	-103.2
WT02	2.0	-88.0[dBw]	-104.3	-102.1	-100.2	-99.6	-99.6	-101.1
WT03	1.0	-78.0[dBw]	-96.5	-97.2	-98.9	-99.9	-101.7	-102.9
WT03	2.0	-88.0[dBw]	-103.9	-101.7	-99.9	-99.3	-99.4	-100.9
WT04	1.0	-78.0[dBw]	-96.6	-97.3	-99.1	-100.1	-101.8	-103.1
WT04	2.0	-88.0[dBw]	-104.1	-101.9	-100.1	-99.4	-99.5	-101.1

B.2.6 WT RCS 35 dBsm

WT	Beam	Reference	500m	1000m	1500m	2000m	3000m	4000m
WT01	1.0	-74.0[dBw]	-96.7	-97.4	-99.2	-100.1	-101.9	-103.2
WT01	2.0	-83.0[dBw]	-104.2	-102.0	-100.2	-99.5	-99.6	-101.1
WT02	1.0	-74.0[dBw]	-96.8	-97.4	-99.2	-100.1	-101.8	-103.2
WT02	2.0	-83.0[dBw]	-104.3	-102.1	-100.2	-99.6	-99.6	-101.1
WT03	1.0	-73.0[dBw]	-96.5	-97.2	-98.9	-99.9	-101.7	-102.9
WT03	2.0	-83.0[dBw]	-103.9	-101.7	-99.9	-99.3	-99.4	-100.9
WT04	1.0	-73.0[dBw]	-96.6	-97.3	-99.1	-100.1	-101.8	-103.1
WT04	2.0	-83.0[dBw]	-104.1	-101.9	-100.1	-99.4	-99.5	-101.1

C. Parameters RCM

C.1 Saint-Hubert